

1 **SurgAI3.8K: a labelled dataset of gynaecologic organs in laparoscopy,**
2 **with application to automatic augmented reality surgical guidance**

3
4
5 **Running title:** SurgAI3.8K laparoscopic image dataset

6 **Title:** SurgAI3.8K: a labelled dataset of gynaecologic organs in laparoscopy, with application
7 to automatic augmented reality surgical guidance

8 **Author names and affiliations:** Sabrina Madad Zadeh M.D. (1,2), Tom François Ph.D.
9 (2), Aurélie Comptour Ph.D. (3), Michel Canis M.D. Ph.D. (2,3), Nicolas Bourdel M.D.
10 Ph.D. (2,3) and Adrien Bartoli Ph.D. (2,4)

- 11 1. Surgical Oncology Department, Centre Jean Perrin, 63011 Clermont-Ferrand, France
12 2. EnCoV, Institut Pascal, UMR 6602 CNRS/Université Clermont-Auvergne, Clermont-
13 Ferrand, France
14 3. Department of Obstetrics and Gynecology, University Hospital Clermont-Ferrand,
15 63000 Clermont Ferrand, France
16 4. Department of Clinical Research and Innovation, University Hospital Clermont-
17 Ferrand, 63000 Clermont Ferrand, France

18 **Corresponding author:** Nicolas Bourdel. nicolas.bourdel@gmail.com. Department of
19 Obstetrics and Gynecology, University Hospital Clermont-Ferrand, 63000 Clermont Ferrand,
20 France. +33676713113

21 **IRB:** IRB 2016-002773-35

22 **Précis:** We provide the surgical dataset SurgAI3.8K, train an Artificial Intelligence system to
23 recognise gynaecologic organs and show its direct impact in an augmented reality surgical
24 guidance software.

25

26 **Abstract**

27 **Study Objective:** We focus on explaining the concepts underlying Artificial Intelligence (AI),
28 using Uteraug, a laparoscopic surgery guidance application based on Augmented Reality
29 (AR), to provide concrete examples. AI can be used to automatically interpret the surgical
30 images. We are specifically interested in the tasks of uterus segmentation and uterus
31 contouring in laparoscopic images. A major difficulty with AI methods is their requirement for
32 a massive amount of annotated data. We propose SurgAI3.8K, the first gynaecological dataset
33 with annotated anatomy. We study the impact of AI on automating key steps of Uteraug.

34 **Design:** We constructed the SurgAI3.8K dataset with 3800 images extracted from 79
35 laparoscopy videos. We created the following annotations: the uterus segmentation, the uterus
36 contours and the regions of the left and right fallopian tube junctions. We divided our dataset
37 into a training and a test dataset. Our engineers trained a neural network from the training
38 dataset. We then investigated the performance of the neural network compared to the experts
39 on the test dataset. In particular, we established the relationship between the size of the
40 training dataset and the performance, by creating size-performance graphs.

41 **Setting:** University

42 **Patients:** NA

43 **Intervention:** NA

44 **Measurements and main results:** The size-performance graphs show a performance
45 plateau at 700 images for uterus segmentation and 2000 images for uterus contouring. The

46 final segmentation scores on the training and test dataset were 94.6% and 84.9% (the higher,
47 the better) and the final contour error were 19.5% and 47.3% (the lower, the better). These
48 results allowed us to bootstrap Uteraug, achieving AR performance equivalent to its current
49 manual setup.

50 **Conclusion:** We describe a concrete AI system in laparoscopic surgery with all steps from
51 data collection, data annotation, neural network training, performance evaluation, to final
52 application.

53 **Keywords:** *artificial intelligence, deep learning, laparoscopic surgery, gynaecological surgery,*
54 *augmented reality, computer-assisted surgery*

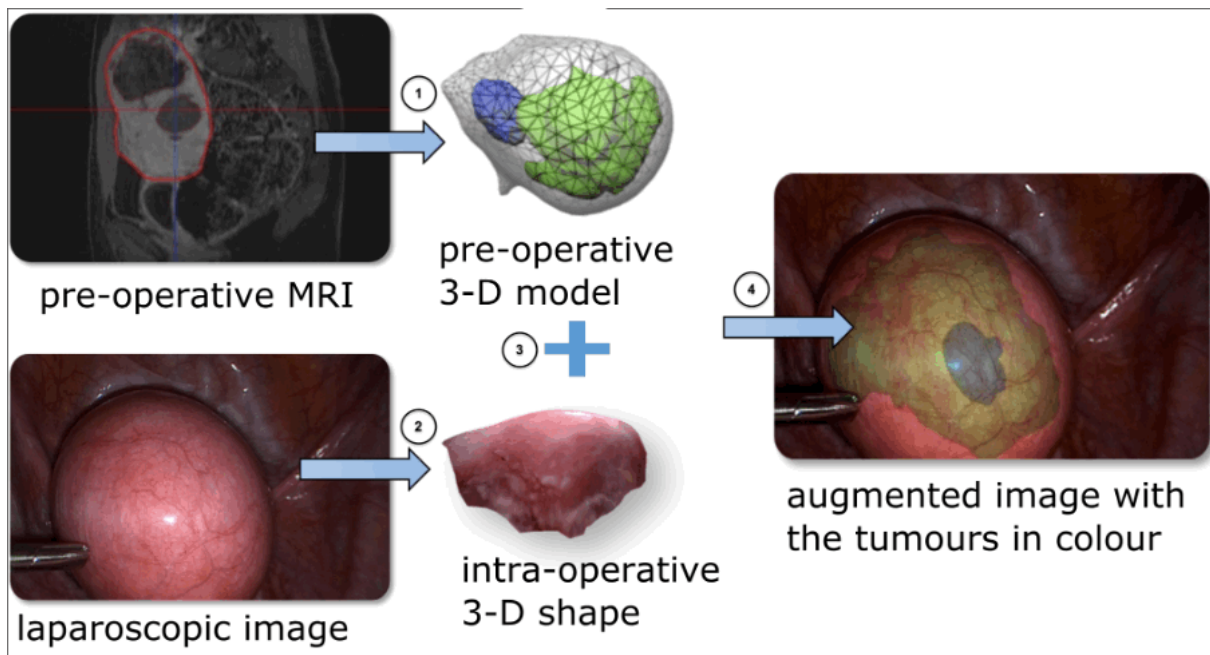
55

56 **1. Introduction**

57 Computer-aided surgery systems require the computer to interpret surgical images
58 automatically. In this respect, Artificial Intelligence (AI) has recently shown unprecedented
59 performance in the technical literature, in particular via the deep learning approach (1). The
60 key idea in deep learning is to train a neural network to replicate results created by experts. A
61 neural network is an artificial object created in the computer's memory¹. The concept of
62 training can be understood as 'teaching', as it is also said that the neural network 'learns from
63 data'. This indeed works by means of creating a dataset, which is an ensemble of images,
64 where the expected results were manually annotated by experts. Our objective is to explain
65 these concepts in detail using a concrete example of surgical application. Specifically, we
66 show that a neural network can be used to automate Uteraug, a visual guidance software for
67 gynecologic surgery developed by our team (2). This article results from the collaboration

¹ A neural network is an artificial object which solves a specific task. Alternatively, the expression neural networks may be found in the literature to encompass the set of methods related to deep learning.

68 between three expert surgeons (SMZ, MC and NB) and two scholars researching and
69 engineering the techniques of AI and their application to surgery (TF and AB).

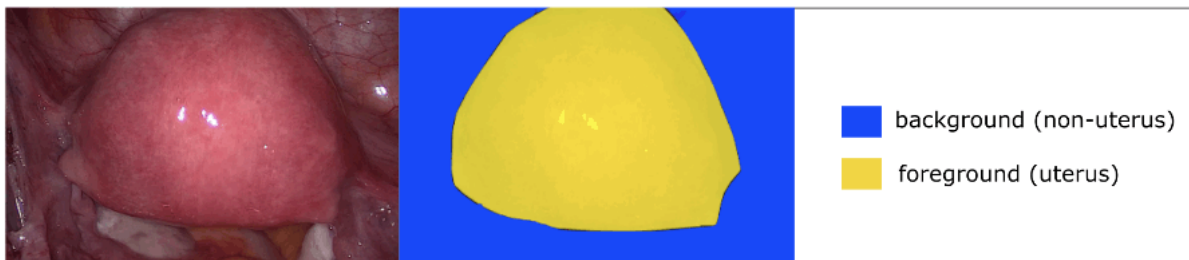


70

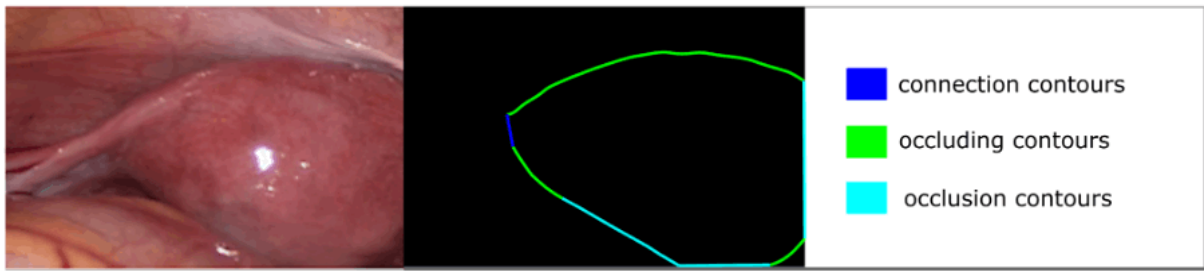
71 **Figure 1: Sketch-up of Uteraug, the EnCoV team's AR system (4).** Example of a
72 laparoscopic myomectomy assisted by AR. Step 1: the preoperative 3D model is
73 reconstructed from pelvic MRI. Step 2: the intraoperative 3D model is reconstructed from a
74 set of laparoscopy images. Step 3: the deformation between the pre- and intraoperative states
75 of the uterus is computed. Step 4: the uterus is tracked automatically and augmented in real
76 time with two myomas using custom colours, creating the effect of virtual transparency. Our
77 proposed neural network has been the cornerstone to automate steps 2 and 4, dropping the
78 need for surgeon attention to setup the system and dramatically increasing usability. In the
79 longer run, our dataset and methods may be used to solve other problems in the
80 implementation of computer-aided surgery support systems. With this in mind, we have
81 included extra annotations in our dataset, namely the junctions between the uterus and
82 fallopian tubes.

83

84 As we shall see, automating Uteraug requires us to solve two tasks. Uteraug implements a
85 virtual transparency visualisation mode of the uterus by fusing preoperative 3D images with
86 the laparoscopic images, as shown in figure 1. In its setup, Uteraug requires the surgeon to
87 select the region occupied by the uterus and its contours in several laparoscopy images, which
88 is a strong limitation in terms of clinical usability. In the context of AI, these two tasks are
89 referred to as *uterus segmentation* and *uterus contouring*, which are illustrated in figures 2
90 and 3. Uterus segmentation consists in labelling each image pixel as being uterus or non-
91 uterus. Uterus contouring consists in labelling each image pixel as being uterus contour or
92 non-contour. Technically, a contour is a boundary between the image part containing the
93 uterus and the rest of the image. These two tasks are extremely simple to solve for an expert
94 in most cases. The human brain is indeed particularly well-equipped to recognise and
95 delineate objects from images. However, in spite of its simplicity, labelling the extent of all
96 pixels in an image is extremely time-consuming for an expert. A major advantage of a neural
97 network is that, once properly trained, it can solve this type of task in a split second, typically
98 processing several dozen images in a second, without any further expert supervision.



100 **Figure 2: Uterus segmentation.** Each image pixel receives one of two labels, namely uterus
101 and non-uterus. The result is called a segmentation mask and is a binary image, which can
102 be visualised with black and white or any other two colours.



103

104 **Figure 3: Uterus contouring.** Each image pixel receives one of four labels, namely occluding
 105 contour (the visible boundaries of the uterus), occlusion contour (for instance, the boundary
 106 created by the sigmoid colon in front of the uterus), connection contour (the connection
 107 between occluding and occlusion contours) and non-contour. The result is called a contour
 108 mask and is a four-colour image, which can be visualised using any four colours. The uterus
 109 contouring task is to achieve the automatic detection of each type of contour.

110

111 A major difficulty with neural networks is their requirement for a massive amount of manually
 112 annotated data (3) to be trained for a specific task. Such data are gathered in a so-called
 113 dataset, which in practice requires surgeons to record surgeries and organise for experts to
 114 label the images. This requires attention and time, making existing datasets extremely
 115 valuable. We propose SurgAI3.8K, the first large gynaecologic dataset, comprising 3800
 116 labelled images. A very important question, which is regularly asked when creating neural
 117 networks, regards the required quantity of data; otherwise said, the minimal size of the dataset
 118 required to achieve the desired task with the expected performance. It has been verified
 119 empirically that for most tasks, the larger the dataset, the better the performance. However,
 120 data is expensive, both in terms of collection and annotation. A sound way of determining
 121 when to stop data collection is to monitor the quantitative performance of the neural network
 122 as the dataset is being collected and annotated. Observing that the performance plateaus,
 123 and if the performance is sufficient for the target application, is generally a reasonable
 124 indication that data collection can be stopped. We show experimentally that our dataset

125 SurgAI3.8K is large enough to train a neural network with reliable performances for uterus
126 segmentation and uterus contouring.

127 Finally, our neural network is shown to be a successful replacement of the surgeon for the
128 manual tasks in Uteraug.

129 **2. Methods**

130 2.1. General Points

131 2.1.1 Deep Learning and Neural Networks

132 Deep learning is the scientific field which deals with large neural networks. A specificity of
133 neural networks is that they do not require one to program the computer to explicitly perform
134 a task. Rather, the neural networks are trained from a dataset containing information about
135 the task, similarly to a human being taught to perform a task from examples. Indeed, the most
136 common training paradigm is called *supervised training*, which requires the dataset to contain
137 examples with their expected results. Training is generally a long process, requiring heavy
138 computational power and the attention of expert engineers. However, it needs to be done only
139 once, representing the first phase in the life cycle of a neural network. The second phase is
140 called *prediction*. At this phase, the neural network is simply used to solve the target task for
141 any new image used at input. The two essential phases to create and use a neural network
142 are thus summarised as follow:

- 143 ● Phase 1: training - the neural network is trained from many examples showing how the
144 target task is solved by experts.
- 145 ● Phase 2 : prediction - the neural network is used to predict the result, in other words to
146 solve the task, for new cases without requiring the attention of experts.

147 The remainder of this paragraph formalises the concept of supervised training. It is slightly
148 technical and may be skipped on a first reading. Formally, we denote an input as X -in the

149 case at hand, X is a laparoscopy image- and the expected result as Y -in the case at hand,
150 we choose Y to be the uterus segmentation for simplicity. The neural network is modelled by
151 a mathematical function f , which has a fixed mathematical form representing the neural
152 network designed by the engineer. Specifically, the neural network design specifies the
153 number of artificial neurons being used and the way they are connected, similarly to biological
154 neurons. Function f takes X as input and maps it to Y . A neural network with some prescribed
155 architecture can be trained to solve many different tasks. This is because its behaviour is
156 controlled by a set of parameters, contained in a variable p , which defines the firing rate of
157 each of the artificial neurons the neural network is made of, again, similarly to biological
158 neurons. Therefore, function f not only depends on X but also on p . The training process
159 attempts to capture the relationship that exists between a laparoscopy image and a uterus
160 segmentation by finding an optimal value for p . Technically, it finds the parameters in p which
161 minimise the distance between Y , which is the expected uterus segmentation from the expert,
162 and $f(X,p)$, which is the prediction of uterus segmentation made by the neural network for a
163 given laparoscopy image X and parameters p . More specifically, the training process
164 estimates p from the whole training dataset, generally containing many pairs (X,Y) of input
165 laparoscopic image and expected uterus segmentation. Once p has been estimated from the
166 training phase, the neural network is ready to be used on new data. This is the prediction
167 phase, whereby the parameters p are frozen and the function $f(X,p)$ used to predict the uterus
168 segmentation Y from a new, previously unseen, input laparoscopy image X .

169 The specificity of deep learning within the general world of machine learning and AI is related
170 to the design of the neural networks it uses. These neural networks are based on artificial
171 neurons, organised in layers connected to each other. The 'deep' qualifier comes from the
172 large number of such layers, forming a so-called deep neural network. The neural network
173 design defines its structure and its number of layers; it is also called the *neural network*
174 *architecture* in the technical literature. The choice of the neural network architecture is critical

175 to obtain reliable results. The architecture we chose for uterus segmentation and uterus
176 contouring is discussed in section 2.2.

177 2.1.2 Annotation and Dataset Size

178 The annotations represent the expected results of the tasks that the neural network should
179 learn, in other words, they are examples used to teach the neural network's purpose. The
180 annotation process is generally carried out manually. For common objects, the annotation can
181 be done by anyone. In the medical field however, the required level of expertise reduces the
182 number of reliable labellers. So, on the one hand, annotating data is time-consuming and on
183 the other hand, the larger the training dataset, the better the final neural network performance.
184 Determining the optimal size of the dataset is thus critical in practice, to best compromise
185 feasibility and performance. We have proposed a methodology to address this problem based
186 on creating a size-performance graph, described in section 2.3.1.

187 2.2. Architecture Design

188 The tasks at hand -uterus segmentation and uterus contouring- are strongly related.
189 Specifically, knowing the segmentation is a strong cue to solve contouring, while knowing the
190 contours should directly allow one to deduce the segmentation, as the inner part of the closed
191 contours. Therefore, a natural question is whether we should strive to solve both tasks, or
192 solve just contouring. Theoretically, this is a sound question, but in practice the contours are
193 not guaranteed to be closed due to imperfect annotations and predictions, as seen for instance
194 in the case of figure 3. Nevertheless, it remains true that both tasks are strongly related. This
195 fact will be exploited by our technical solution, which uses a neural network architecture
196 solving both tasks simultaneously. More specifically, our engineers chose an existing neural
197 network architecture well-adapted to medical images called U-Net (4) and specialised it to the
198 tasks at hand. In short, the proposed neural network has the following input and output
199 specificities:

- 200 • Neural network inputs: the laparoscopy image.
- 201 • Neural network outputs: the segmentation and the contours.

202 The proposed methodology is applicable to any dataset containing contour annotations,
203 whether it be a dataset of surgical images or other modalities such as radiological images.

204 2.3. Dataset Creation and Neural Network Training

205 2.3.1 Dataset Size

206 Finding the optimal dataset size is a challenging question because, as we have seen, it
207 represents a trade-off between labelling effort and performance. The relationship to
208 performance is easy to understand: an object has a visual appearance depending on several
209 factors, including its position with respect to the camera and the background it lies on. The
210 larger the number of examples which the neural network learns from, the better it will
211 extrapolate to new data. However, beyond a certain quantity of examples, the addition of new
212 examples will only lead to a marginal performance gain which is probably not worth the
213 labelling effort. Hence, an optimal dataset size may be found as the best compromise between
214 the labelling manpower availability and cost, and the incremental performance gain.

215 We propose to determine an optimal dataset size for uterus segmentation and uterus
216 contouring by studying size-performance graphs. We measure performance using the so-
217 called *test error*. The test error is an extremely simple, yet important notion. Once the neural
218 network is trained, the test error is computed from the test dataset, containing data
219 independent of the training dataset. In other words, the test error uses images which were not
220 used for training, and for which the expected results are available, to compare the prediction
221 of the neural network against the expert. It is thus customary for the engineers to split the
222 dataset in two parts: the training dataset, which is typically about 80% of the dataset, which is
223 used to train the neural network, and the test dataset, which is typically about 20% of the
224 dataset, which is used to evaluate the performance independently.

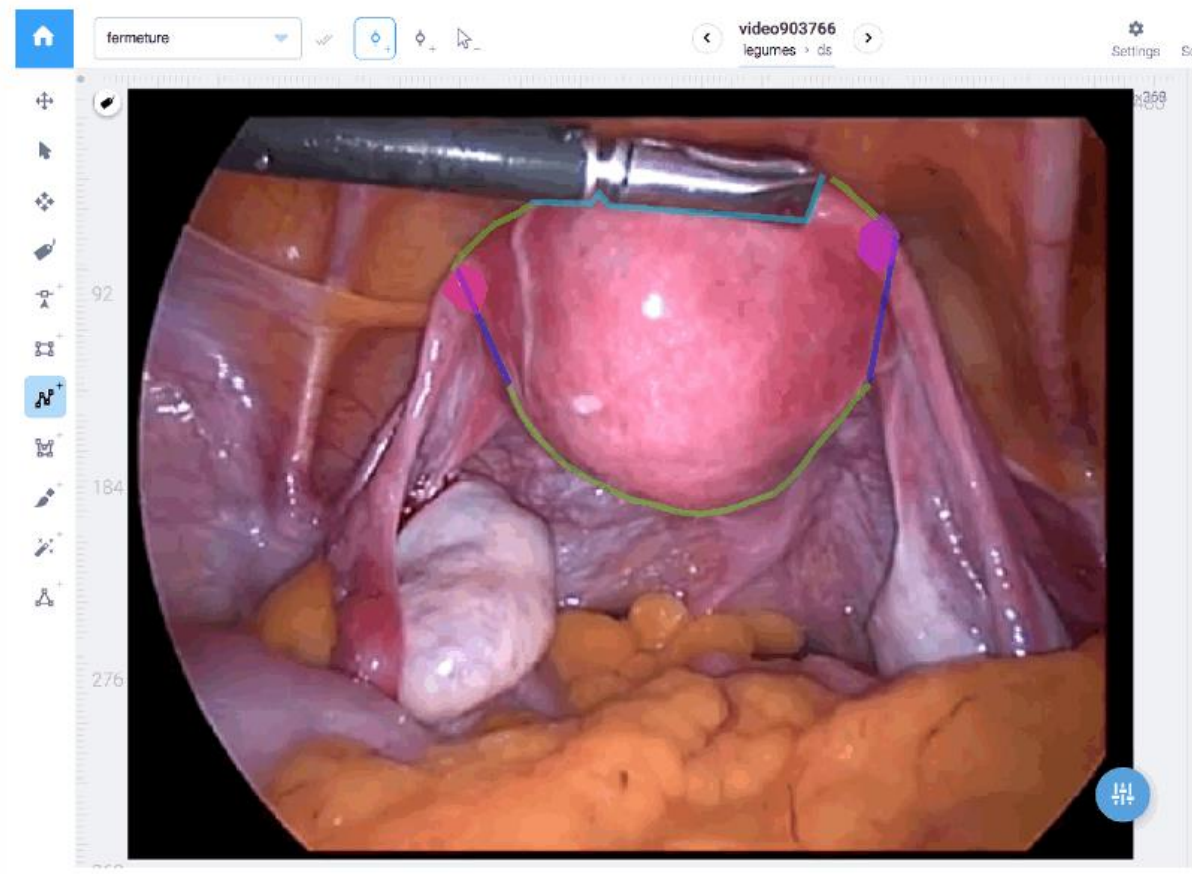
225 Our methodology to construct the size-performance graphs is to train the neural network
226 incrementally. We start with a small subset of the dataset of size 100 images, train the neural
227 network and measure its performance. We then add a batch of 100 images to the training
228 dataset and repeat the steps. We thus obtain the sought size-performance graph, into which
229 we search for a performance plateau. The test dataset used to measure performance is fixed.
230 It contains 581 images, representing approximately 15% of our 3800 images. The test and
231 training datasets contain images from different procedures to prevent any patient overlap and
232 to guarantee an unbiased performance evaluation.

233 2.3.2 Data Source, Extraction and Selection

234 We construct SurgAI3.8K, our proposed dataset, by extracting and labelling individual frames
235 from 79 laparoscopy videos. The videos were recorded as part of a research protocol (IRB
236 2016-002773-35) (6,7). When creating a dataset, it is crucial to ensure data diversity. The
237 dataset should be large, but it should also span the possible usage conditions. We have taken
238 care of using videos capturing both intra-patient and inter-patient diversity. Intra-patient
239 diversity is covered by including images with various uterus viewpoints, deformations and
240 colour, as the latter evolves through the procedure. Inter-patient diversity is simply covered by
241 including videos from different patients. In addition, we used videos from three types of
242 procedures: hysterectomy, laparoscopic fertility exploration and endometriosis surgeries
243 containing images of both normal and pathological cases. We used 79 videos from which we
244 extracted our dataset of 3800 images. Technically, the videos were visualised with the
245 multimedia player VLC, which allowed us to extract images at a regular time interval. The final
246 images were then manually selected in order to fulfil the above diversity criteria. Manual
247 selection by an expert is very important: it favours quality and diversity, whereas an automatic
248 selection, for instance directly using the images extracted at a regular time interval, would
249 focus on quantity only.

250 2.3.3 Annotation, Tools and Labellers

251 In our dataset, the annotations were designed to resolve uterus segmentation and uterus
252 contouring. The uterus contours identify the relationships between the uterus and its
253 neighbouring organs in terms of visual occlusions. Specifically, each of the pixels forming the
254 uterus contours can be of one of three types: the occluding contour type, where the uterus
255 ends by occluding another organ, the occlusion contour type, where the uterus is occluded by
256 another organ or the image boundaries, and the connection contour type, where the uterus is
257 connected to another organ. We have also labelled the junctions between the uterus and
258 fallopian tubes specifically, to allow further usage. Overall, we thus specifically have the
259 following annotations for each image of our dataset: the uterus segmentation, the uterus
260 occluding contours, the uterus occlusion contours, the uterus connection contour, the region
261 of the right fallopian tube junction and the region of the left fallopian tube junction. These
262 annotations can be combined and arranged to create new labels. For instance, the fallopian
263 tube junction region can be used together with the connection contour mask to create the
264 uterus-fallopian tube junction mask. The selected images were transferred to the online
265 annotation software Supervise.ly (8). They were then annotated by two expert gynaecological
266 surgeons (SMZ and NB). Figure 4 shows an example of an annotated image under
267 Supervise.ly.



268

269 **Figure 4: Example of a laparoscopic image annotated with the online annotation**
270 **software, Supervise.ly.** In green, the occluding contours, in light blue the occlusion contours,
271 in dark blue the connection contours and in purple and pink the right and left uterus-fallopian
272 tube junctions.

273

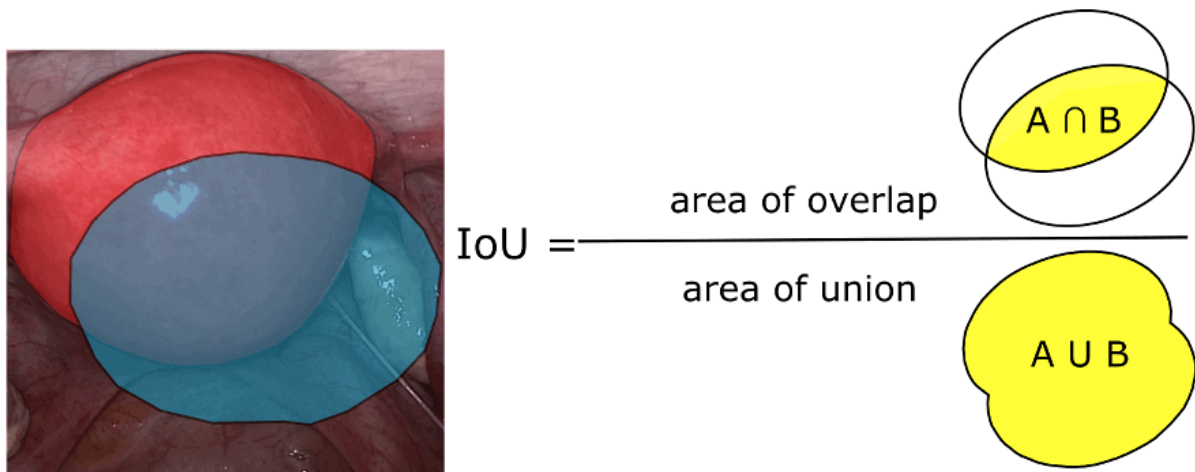
274 3. Results

275 3.1 Neural Network Implementation and Evaluation

276 Our engineers (TF and AB) implemented the neural network using the programming language
277 Python with *Facebook's PyTorch software toolbox* running on a standard desktop PC
278 computer. They evaluated the neural network with so-called evaluation metrics, quantifying
279 the discrepancy between the predicted and the expert annotations, for the images from the

280 test dataset. Recall that the test dataset contains patient data which were not used to train the
281 neural network. It thus allows one to perform an independent evaluation. We now describe the
282 evaluation metrics.

283 *Uterus segmentation.* Segmentation is a well-studied task for which there exist simple and
284 commonly accepted evaluation metrics. Specifically, we use the Intersection over Union (IoU),
285 which vastly dominates the evaluation of segmentation in the literature. As illustrated in figure
286 5, the IoU represents the percentage of overlap between the expert segmentation and the
287 neural network predicted segmentation. We use the average of the IoU over all the images
288 from the test dataset. The IoU is a measure of agreement between the experts and the neural
289 network, thus the higher, the better. The IoU ranges from 100%, which is a perfect result, to
290 0%, which is a very bad result.



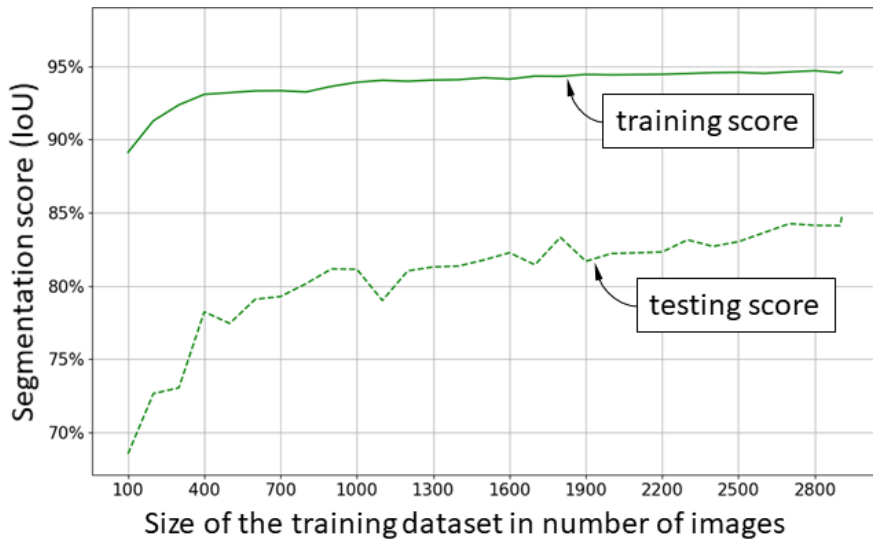
292 **Figure 5: Intersection over Union explanatory diagram.** The IoU between segmentations
293 A and B is defined as the ratio between the area of the intersection and the area of the union
294 of A and B. In the example image, A in red is the expert segmentation and B in blue is the
295 neural network predicted segmentation, leading to an IoU of 39%. The IoU is usually
296 expressed as a percentage and varies between 100% for a perfect segmentation and 0% for
297 an extremely poor segmentation.

298

299 *Uterus contouring*. In contrast to segmentation, the evaluation metric for contour detection is
300 challenging to design and has not been standardised yet. This is because a contour is a
301 precisely localised thin image part. A prediction is thus rarely perfect, in the sense that it never
302 perfectly reproduces the annotation. Consequently, even if a prediction lies close to the
303 annotation and is thus acceptable, it will in most cases have a very low IoU. Our engineers
304 proposed the *contour error*, which addresses the problem using a tolerance distance between
305 the contour points, as explained in our previous paper (5). The final contour error is a measure
306 of discrepancy between the experts and the neural network, thus the lower, the better. The
307 contour error ranges from 0%, which is a perfect result, to 100%, which is a very bad result.

308 3.2 Training Results and Dataset Size

309 The dataset consists of 3800 annotated images, whose characteristics are given in table 1.
310 The dataset was split into a training set of 3234 images and a test set of 581 images. Figure
311 6 shows the uterus segmentation performance. We observed a steep improvement from 100
312 to 700 training images and a much slower improvement beyond. The final IoU on the training
313 and test datasets were 94.6% and 84.9% (the higher, the better). Similarly, for uterus
314 contouring, we observed a steep improvement from 100 to about 2000 training images and a
315 much slower improvement beyond. The final contour error on the training and test datasets
316 were 19.5% and 47.3% (the lower, the better).



317

318 **Figure 6: Size-performance graphs for uterus segmentation and uterus contouring.** The
 319 curves show the performance as the training set is increased by adding batches of 100
 320 images. Recall the higher, the better for the segmentation score (the IoU) and the lower, the
 321 better for the contour error.

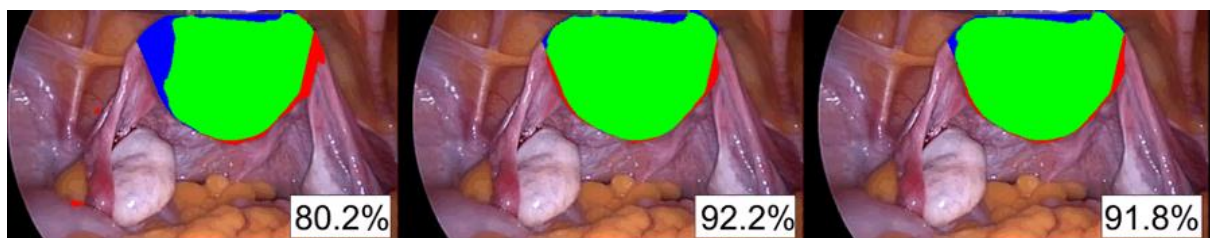
322

The dataset	
Data	images
Number of patients	79
Number of videos	79
Laparoscopic gynaecological procedures	Hysterectomies (48) Rectovaginal endometriosis nodule (21) Laparoscopic fertility exploration (10)
Classes	Uterus segmentations (3800) Occluding contours (3809) Occlusion contours (2629) Closure contours (3711) Left uterus-fallopian tube junction (1364) Right uterus-fallopian tube junction (1368)

323

324 **Table 1. Characteristics of the proposed SurgAI3.8K dataset.**

325 Figure 7 illustrates the uterus segmentation results for the cases of 100, 1300 and 2900
 326 training images. Visual inspection confirms that, as suggested by the IoU values, while a
 327 strong agreement holds between the second and third cases, a substantial difference can be
 328 seen between them and the first case.



329

330 **Figure 7: Uterus segmentation results.** Training was performed with (a) 100, (b) 1300 and
 331 (c) 2900 images. True Positives are in green, i.e. pixels labelled as 'uterus' by the expert and
 332 predicted as 'uterus' by the neural network, False Positives are in red, i.e. pixels not labelled
 333 as 'uterus' by the expert and predicted as 'uterus' by the neural network and False Negatives
 334 are in blue, i.e. pixels labelled as 'uterus' by the expert and not predicted as 'uterus' by the
 335 neural network. The IoU is given in the bottom right corner.

336

337 Figure 8 illustrates the occluding contours of the uterus for the cases of 100, 1300 and 2900
338 training images. Visual inspection confirms that, as suggested by the contour error, while a
339 strong agreement holds between the second and third cases, a substantial difference can be
340 seen between them and the first case.

341



342

343 **Figure 8: Uterus contouring results.** The images specifically show the occluding contours
344 of the uterus. Training was performed with (a) 100, (b) 1300 and (c) 2900 images. True
345 Positives are in green, i.e. pixels labelled as 'occluding contour' by the expert and predicted
346 as 'occluding contour' by the neural network, False Positives are in red, i.e. pixels not labelled
347 as 'occluding contour' by the expert and predicted as 'occluding contour' by the neural network
348 and False Negatives are in blue, i.e. pixels labelled as 'occluding contour' by the expert and
349 not predicted as 'occluding contour' by the neural network. The contour error is given in the
350 bottom right corner.

351

352 4. Discussion

353 4.1 Summary of Contributions

354 *Introducing the method of AI.* This article contributed a pedagogical introduction of the
355 fundamental notions of AI, through the use of a concrete application of image processing
356 towards automating a surgery guidance application, as described below. It introduced the

357 notions of neural networks, their design, their training from the training dataset and their
358 performance evaluation from the test dataset. It then shows that the key factor is the availability
359 of a dataset with expert annotations. This introduction is intended to give surgeons an
360 understanding of how AI works and the ability to use it wisely. For instance, it is clear that if a
361 neural network was not trained on a sufficiently large dataset, its performance may be poor in
362 some cases. Requesting the amount of cases a neural network was trained from and what the
363 test error was may thus become a natural question for the surgeons to ask before adopting an
364 AI-based technology.

365 *The dataset.* This work contributed to the construction of a dataset of annotated laparoscopic
366 images for the uterus segmentation, uterus contouring and fallopian tube junctions detection
367 tasks. Compared to the existing datasets for the automatic recognition of common, non-
368 medical objects, it is modest in size. Nonetheless, it has variability, obtained by including
369 multiple patients, different times of surgery, different view angles, and has quality manual
370 annotations. Several datasets for the automatic detection of surgical tools exist in the
371 literature, but very few works deal with the automatic detection of anatomical structures. Prior
372 to this work, we carried out a feasibility study on a reduced dataset and a simple task of
373 detecting pelvic organs (uterus, ovary, surgical tools) (9). This prior work showed that AI
374 techniques could feasibly solve this type of task. Leibetseder et al. have carried out several
375 studies in laparoscopic surgery, but their work focuses on the classification of surgical images
376 (10), merely indicating the presence or absence of an organ in an image. Recently, they have
377 published work aiming at endometriosis detection in laparoscopic surgery images (11). They
378 have published a dataset of 25K images with half of the images with endometriosis lesions
379 and the other half without. Only 300 images are manually annotated with specific
380 endometriosis lesion contours, which are known to require a high degree of expertise in
381 laparoscopic anatomy. More recently, the same team has published endometriosis lesion
382 detection using Mask-RCNN (12), which was a significant step forward. Concretely, the results
383 are bounding boxes containing the lesions. In contrast, our results provide the detailed contour

384 of the anatomical structures, representing a much richer piece of information than a bounding
385 box. In addition, several studies have been carried out on the automatic detection of surgical
386 tools (13–15). Surgical tools differ significantly from the abdominal anatomy and do not
387 necessarily require expert annotation. There is no large-scale dataset for the automatic
388 detection of gynaecological organs in laparoscopic surgery to date. Nevertheless, the
389 proposed dataset could be extended by labelling the other anatomical structures visible in the
390 image, which may potentially improve the performance of AI. We leave this extension for future
391 work.

392 *Dataset size.* An important contribution of this work is to analyse the size of the laparoscopic
393 image dataset required for the automatic segmentation and contouring of the uterus in a
394 laparoscopic image. It contributes to answering an essential question regarding the use of AI
395 techniques, which regards the number of training images necessary and sufficient to achieve
396 the desired performance. This question has not been resolved to date in the literature. We
397 bring an answer regarding uterus segmentation and contouring by means of observing the
398 size-performance graphs. We may hypothesise that for other organs presenting the same type
399 of inter-patient variability on a laparoscopic image, it may be possible to consider the creation
400 of a dataset with the same order of magnitude in size to obtain similar results.

401

402 4.2 Contribution of the Neural Network to Augmented Reality

403 The objective of solving uterus segmentation and uterus contouring was to replace the manual
404 annotation required at the initialisation phase of Uteraug, the AR based laparoscopic surgery
405 assistance software developed by our team in prior work. Steps 2 and 4 in the initialisation
406 phase include manual interactions: the selection of the region formed by the image of the
407 uterus and the selection of the different contours of the uterus. Thanks to our dataset and
408 trained neural network, we have automatized these manual tasks. We have integrated our
409 neural network to Uteraug and evaluated the quality of the manual and automatic solutions by

410 comparing the surgeons' annotations with the neural network. We have also measured the
411 time saved by the automatic annotation during the initialisation phase. These results have
412 been published by our team in (6). The automatic annotation achieves almost identical AR
413 results to manual annotation in terms of quality. The time is reduced by 3 minutes and 56
414 seconds compared to manual annotation, on average, which represents a 97.4% reduction,
415 increasing the software usability and presumably its acceptability. The manual interactions
416 required at the initialisation phase of Uteraug would harm its clinical use in the operating room
417 without trained staff. By automating this phase, AI offers the possibility to extend its use to a
418 larger number of surgeons.

419 **5. Conclusion**

420 We have described a concrete example of how AI can be used in surgery, which conveys the
421 basic concepts of AI in a pedagogical way, with illustrations given on the concrete case of
422 augmented reality in laparoscopy.

423

424 Disclosures: Drs Sabrina Madad Zadeh, Tom Francois, Aurélie Comptour, Michel Canis,
425 Nicolas Bourdel and Adrien Bartoli report no conflict of interest.

426 Source of funding: no funding

427 **References:**

- 428 1. Sermanet P, Eigen D, Zhang X, Mathieu M, Fergus R, LeCun Y. OverFeat: Integrated
429 Recognition, Localization and Detection using Convolutional Networks. ArXiv13126229 Cs
430 [Internet]. 23 févr 2014 [cité 20 sept 2020]; Disponible sur: <http://arxiv.org/abs/1312.6229>
- 431 2. Collins T, Pizarro D, Gasparini S, Bourdel N, Chauvet P, Canis M, et al. Augmented Reality
432 Guided Laparoscopic Surgery of the Uterus. IEEE Trans Med Imaging. janv
433 2021;40(1):371-80.

- 434 3. Goodfellow I, Bengio Y, Courville A. Deep Learning. Cambridge, MA, USA: MIT Press;
435 2016. 800 p. (Bach F. Adaptive Computation and Machine Learning series).
- 436 4. Ronneberger O, Fischer P, Brox T. U-Net: Convolutional Networks for Biomedical
437 Image Segmentation. In: Navab N, Hornegger J, Wells WM, Frangi AF, éditeurs. Medical
438 Image Computing and Computer-Assisted Intervention – MICCAI 2015. Cham: Springer
439 International Publishing; 2015. p. 234-41. (Lecture Notes in Computer Science).
- 440 5. François T, Calvet L, Madad Zadeh S, Saboul D, Gasparini S, Samarakoon P,
441 et al. Detecting the occluding contours of the uterus to automatise augmented laparoscopy:
442 score, loss, dataset, evaluation and user study. Int J Comput Assist Radiol Surg. juill
443 2020;15(7):1177-86.
- 444 6. Bar-Shavit Y, Jaillet L, Chauvet P, Canis M, Bourdel N. Use of indocyanine
445 green in endometriosis surgery. Fertil Steril. 1 juin 2018;109(6):1136-7.
- 446 7. Bourdel N, Jaillet L, Bar-Shavit Y, Comptour A, Pereira B, Canis M, et al.
447 Indocyanine green in deep infiltrating endometriosis: a preliminary feasibility study to examine
448 vascularization after rectal shaving. Fertil Steril. août 2020;114(2):367-73.
- 449 8. Supervisely - Web platform for computer vision. Annotation, training and deploy
450 [Internet]. 2020 [cité 20 sept 2020]. Disponible sur: <https://supervise.ly/>
- 451 9. Madad Zadeh S, Francois T, Calvet L, Chauvet P, Canis M, Bartoli A, et al. SurgAI:
452 deep learning for computerized laparoscopic image understanding in gynaecology. Surg
453 Endosc. 29 janv 2020;
- 454 10. Lapgyn4 | Proceedings of the 9th ACM Multimedia Systems Conference [Internet].
455 2020 [cité 20 sept 2020]. Disponible sur:
456 <https://dl.acm.org/doi/abs/10.1145/3204949.3208127>

- 457 11. Leibetseder A, Kletz S, Schoeffmann K, Keckstein S, Keckstein J. GLEND A:
458 Gynecologic Laparoscopy Endometriosis Dataset. In: Ro YM, Cheng WH, Kim J, Chu WT, Cui
459 P, Choi JW, et al., éditeurs. MultiMedia Modeling. Cham: Springer International Publishing;
460 2020. p. 439-50. (Lecture Notes in Computer Science)
- 461 12. He K, Gkioxari G, Dollar P, Girshick R. Mask R-CNN. In 2017 [cité 8 mars 2022]. p.
462 2961-9. Disponible sur: [https://openaccess.thecvf.com/content_iccv_2017/html/He_Mask_R-](https://openaccess.thecvf.com/content_iccv_2017/html/He_Mask_R-CNN_ICCV_2017_paper.html)
463 [CNN_ICCV_2017_paper.html](https://openaccess.thecvf.com/content_iccv_2017/html/He_Mask_R-CNN_ICCV_2017_paper.html)
- 464 13. Zhang B, Wang S, Dong L, Chen P. Surgical Tools Detection Based on Modulated
465 Anchoring Network in Laparoscopic Videos. IEEE Access. 2020;8:23748-58.
- 466 14. EndoVisSub-Instrument - Grand Challenge [Internet]. grand-challenge.org. 2020 [cité
467 20 sept 2020]. Disponible sur: <https://endovissub-instrument.grand-challenge.org/>
- 468 15. García-Peraza-Herrera LC, Li W, Fidon L, Gruijthuijsen C, Devreker A, Attilakos G, et
469 al. ToolNet: Holistically-nested real-time segmentation of robotic surgical tools. In: 2017
470 IEEE/RSJ International Conference on Intelligent Robots and Systems (IROS). 2017. p.
471 5717-22.